HOT-PRESSED DOWELS IN BONDED-IN ROD TIMBER CONNECTIONS

Wen-Shao Chang†

Lecturer
Department of Architecture and Civil Engineering
University of Bath
Bath, United Kingdom
E-mail: wsc22@bath.ac.uk

Nicholas Nearchou

Engineer
Engenuiti Limited
London, United Kingdom
E-mail: nick_nearchou@hotmail.com

(Received November 2014)

Abstract. Bonded-in rod connections are becoming a more and more popular method in the construction industry for connecting timber. These connections are favored for their versatility. The most commonly used system is bonded-in steel rods, which are typically prone to brittle failures. The aim of this study was to investigate the potential of hot-pressed wooden rods as an alternative to conventional steel bonded-in rod systems, which have better material harmonization and exclude the use of adhesives. The proposed connection was applied to the practical situation of a beam splice in flexure to determine its potential. The results showed that ductile failure mode occurred at high rotations at which peak loads were displayed. A theoretical model was developed and found to be accurate compared with the experimental results. This type of connection has good ductility, which suggests its application in domestic timber framing in regions of high seismicity would be practical.

Keywords: Bonded-in rod, timber connection, compressed wood.

INTRODUCTION

Connections within framing are usually the critical points of a structure. The choice of connection type and layout is crucial because it will directly affect the global performance of the structure. The construction industry currently uses conventional bonded-in rods, which often are responsible for unfavorable brittle failures and have poor environmental credentials. Bonded-in rod connections are becoming a popular connecting method because of their versatility, aesthetic qualities, performance, and economic value (Bainbridge and Mettem 1999). In some areas, such as Japan, bonded-in rods are very commonly used in housing and residential construction because of the ease of fabrication and excellent performance (Jung et al 2010). They are also becoming more popular in modern European domestic framing. For example, this system has been manufactured in France and used widely in timber-framed houses (Ansell and Smedley 2007). A wide range of parameters of steel bonded-in rod connections used in timber members under axial loading have been investigated. Tests have been carried out on spacing and edge distance of steel glued-in rod (GIR) connections in timber members under axial load to quantify load carrying capacity (Blass and Laskewitz 1999) and the influence of timber density. Geometric parameters, such as member and rod dimensions, have also been studied to prevent premature splitting of the timber members (Gustafsson et al 2001; Feligioni et al 2003; Steiger et al 2007). The conventional steel bonded-in rod connections are prone to brittle failure in tension or premature splitting because of the disharmonization between the rod and timber in bending (Yeboah et al 2009).

* Corresponding author
† SWST member

Some systems have tried to address this issue. For example, glass-fiber-reinforced polymer (GFRP) bonded-in rods were recommended as an alternative to steel GIR connections because they have better compatibility with parent material and adhesive (Harvey and Ansell 2003). However, GFRP rods are not easy to cut or machine on site, which makes them extremely awkward to recycle when the structures come to the end of their life. Hardwood (Jensen et al 2001) and hot-pressed wooden dowels (Jung et al 2010) are also alternative solutions for tackling the problems of steel GIR connections. Another problem with all existing GIR systems is the use of adhesives. Currently, a two-part epoxy resin is usually used. Structural adhesives including epoxy resin have been associated with causing skin irritation and triggering asthma, which raises health and safety concerns. The use of adhesives requires very good quality control systems. Therefore, connections are very often manufactured off-site. Some adhesives used in an external environment have also been known to leach into the surrounding ecosystem, causing deterioration. There is a gap in the industry for an ecofriendly, recyclable, and nonbrittle alternative to existing GIR systems, which should lead to the development of an all-timber binderless connection. This study proposes a new system, a binderless hot-pressed dowel, to tackle the aforementioned issues and explore the potential for use in a timber-framed structure.

PROPOSED CONNECTION

The hot-pressed timber undergoes a thermal-mechano-hydro process (the timber is densified with high temperature). A number of studies have reported stability of the hot-pressed timber and how it was stabilized (Welzbacher et al 2008; Rautkari et al 2010; Fang et al 2012). Some studies took a different approach by exploiting the swelling properties of hot-pressed wood (Anshari et al 2011, 2012). These studies relied on friction along the dowel–hole interface caused by the expansion of the soaked dowel within the clearance hole. As the dowel expands, it exerts a confining force on the parent timber hole wall (N_{swell}), which then mobilizes a frictional resistance force (F_{mob}) when the dowel is subject to pull-out (P) (Fig 1). With time, the regular timber dowels dry out and shrink, alleviating the confining pressure. However, hot-pressed timber dowels retain a portion of expansion caused by swelling, which addresses this issue. This connection enables harmony between the two materials, which should improve ductile behavior and increase recyclability because of the absence of adhesive and metal. A distinct application could be timber framing in domestic housing, in which the connection can be used for header–stud connections and column splicing.

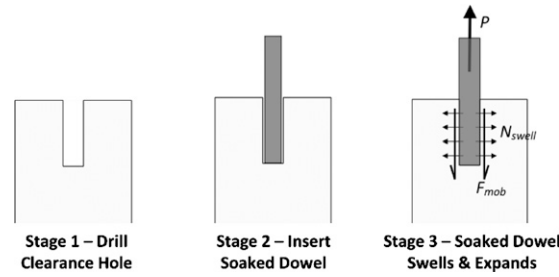

Figure 1. Principle of proposed connection.

ANALYTICAL APPROACH

Figure 2 shows the proposed connection being used as a beam–beam connection under bending. The dowel exhibited flexure (M_d) deformation caused by the beam moment (M_{beam}). The angle of curvature (θ_2) in the dowel may be different from the opening angle of the beam (θ_1) but can be determined using similar triangles and the radius curvature (R_d) as shown in Fig 3:

$$\theta_2 \times R_d = \theta_1 \times D \quad (1)$$

where D is the lever arm depth of the dowel from the beam top, and the angle of opening is θ_1.

The energy dissipated by the dowel in bending ($U_{d,bend}$) is equal to the moment in the dowel (M_d) multiplied by the rotation of the dowel (θ_2). The energy dissipated by flexure can be written as

$$U_{d,bend} = M_d \times \theta_2 \quad (2)$$

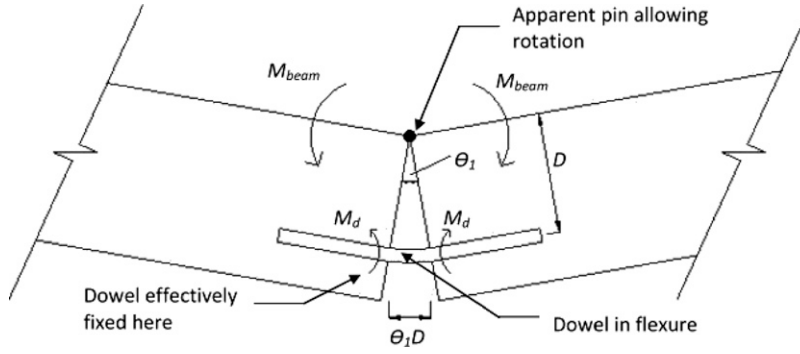

Figure 2. Contribution from dowel in bending.

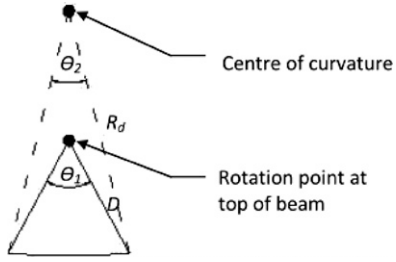

Figure 3. The relationship of curvature and rotation center of beam.

Combining Eqs 1 and 2 gives

$$U_{\mathrm{d,bend}} = \frac{M_{\mathrm{d}}\theta_1 D}{R_{\mathrm{d}}} \tag{3}$$

With regard to dowel slippage, the dowel will mobilize frictional slip resistance (F_{mob}), which will increase joint moment capacity (Fig 4).

The frictional force that can be mobilized is related to the normal force on the side of the parent timber hole wall (N_{tot}) and the coefficient of friction between the dowel and wall (μ):

$$F_{\mathrm{mob}} = N_{\mathrm{tot}} \times \mu \tag{4}$$

The normal force is made up of two components: the force caused by the dowel swelling (N_{swell}) and the forces caused by the moment in the dowel (N_{bend}). Figure 5 shows the stress distribution on the parent timber hole wall caused by the dowel.

The normal force caused by the reaction to the dowel in flexure (N_{bend}) is related to the dowel moment (M_{d}). The couple caused by N_{bend} is a reaction to the moment in the dowel (M_{d}), and both are equal as given:

$$N_{\mathrm{bend}} \times \frac{2}{3} l_{\mathrm{eff}} = M_{\mathrm{d}} \tag{5}$$

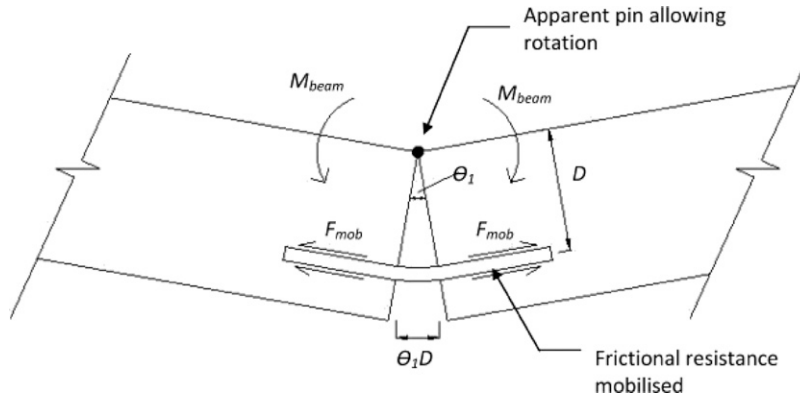

Figure 4. Contribution from dowel slipping.

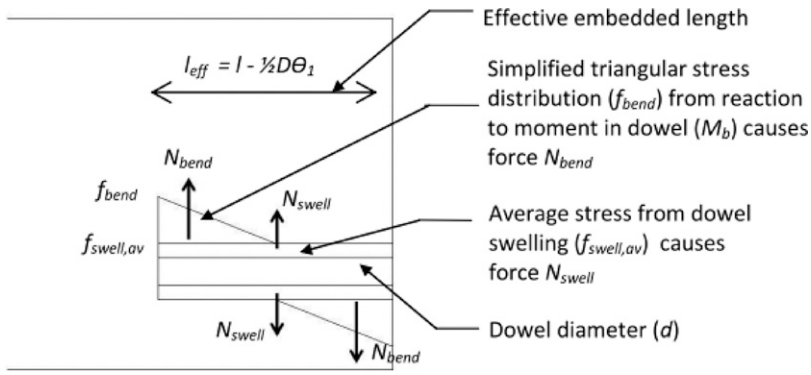

Figure 5. Stress distribution on dowel hole during slippage.

$$l_{\text{eff}} = l - \frac{1}{2}D\theta_1 \tag{6}$$

Combining Eqs 5 and 6 gives

$$N_{\text{bend}} = \frac{3M_{\text{d}}}{2(l - \frac{1}{2}D\theta_1)} \tag{7}$$

The normal force caused by swelling is equal to the swelling pressure (f_{swell}) multiplied by the effective length of the dowel (l_{eff}) multiplied by the effective swelling circumference. The effective swelling circumference is equal to half the normal circumference because the dowel only expands in the radial direction, not tangentially. The normal force caused by swelling can be expressed as

$$\begin{aligned} N_{\text{swell}} &= f_{\text{swell}} l_{\text{eff}} \tfrac{1}{2}\pi d \\ &= \tfrac{1}{2} f_{\text{swell}}(l - \tfrac{1}{2}D\theta_1)\pi d \end{aligned} \tag{8}$$

The total normal force then becomes the bending and swelling components combined, and can be written as

$$N_{\text{tot}} = \frac{3M_{\text{d}}}{2(l - \frac{1}{2}D\theta_1)} + \tfrac{1}{2} f_{\text{swell}}(l - \tfrac{1}{2}D\theta_1)\pi d \tag{9}$$

The total frictional resistance force mobilized (F_{mob}) is then equal to the kinetic coefficient of friction (μ) (because the dowel has already started slipping) multiplied by this normal force (N_{tot}):

$$F_{\text{mob}} = \mu \frac{3M_{\text{d}}}{2(l - \frac{1}{2}D\theta_1)} + \tfrac{1}{2}\mu f_{\text{swell}}(l - \tfrac{1}{2}D\theta_1)\pi d \tag{10}$$

The energy dissipated by the dowel slipping ($U_{\text{d,slip}}$) is equal to the frictional force (F_{mob}) multiplied by the slip displacement of the dowels. Assuming the angles are small, the energy dissipated from slipping can be written as

$$U_{\text{d,slip}} = F_{\text{mob}} \times D\theta_1 \tag{11}$$

Combining Eqs 10 and 11 gives

$$U_{\text{d,slip}} = \mu \frac{3M_{\text{d}} D\theta_1}{2(l - \frac{1}{2}D\theta_1)} + \tfrac{1}{2}\mu f_{\text{swell}} l D\theta_1 \pi d \tag{12}$$

The overall energy dissipated by the connection during bending (U_{tot}) is the two components combined and can be written as

$$\begin{aligned} U_{\text{tot}} = \frac{M_{\text{d}}\theta_1 D}{R_d} &+ \mu \frac{3M_{\text{d}} D\theta_1}{2(l - \frac{1}{2}D\theta_1)} \\ &+ \tfrac{1}{2}\mu f_{\text{swell}} l D\theta_1 \pi d \end{aligned} \tag{13}$$

If we consider conservation of energy, then work done equals the total energy dissipated during failure:

$$\begin{aligned} M_{\text{Rd}}\theta_1 = \frac{M_{\text{d}}\theta_1 D}{R_d} &+ \mu \frac{3M_{\text{d}} D\theta_1}{2(l - \frac{1}{2}D\theta_1)} \\ &+ \tfrac{1}{2}\mu f_{\text{swell}} l D\theta_1 \pi d \end{aligned} \tag{14}$$

Assuming that the angle is small, the moment capacity of beam can be expressed in the form of

$$M_{\text{Rd}} = M_{\text{d}} D\left(\frac{1}{E_{\text{d}} I_{\text{d}}} + \mu \frac{3}{2l}\right) + \tfrac{1}{2}\mu f_{\text{swell}} l D\pi d \tag{15}$$

MATERIALS AND METHODS

Dowel Bending Tests

Western redcedar (*Thuja plicata*) with an average density of 390 kg/m^3 was used to fabricate hot-pressed dowels and as specimens in bending, punching shear, and beam bending tests. To hot-press the timber, the wood specimens were placed between platens that were preheated to 130°C and pressed for 5 min with a compression ratio of 40%. The compression ratio can be defined as

$$C = \frac{R_0 - R_C}{R_0} \times 100[\%] \qquad (16)$$

where R_0 and R_c represent dimension in compression direction before and after compression, respectively.

Four-point bending tests were conducted to establish the mechanical properties of the hot-pressed dowels. To have more reliable results and less variation, a total of 30 hot-pressed specimens were then cut into dimensions of 12 × 12 × 240 mm^3 for bending tests. Specimens prepared for the bending test had average density of 553.2 kg/m^3 with a standard deviation of 62.0 kg/m^3. The effective span between supports was set to 200 mm. All testing procedures and determination of mechanical properties were conducted in compliance with BSI (2011).

Punching Shear Tests

Punching shear tests were conducted to determine the performance of the bond between parent timber and expanded dowel. Clear and small western red cedar samples with dimensions of 23 × 15 × 260 mm^3 were prepared and hot-pressed from 23 to 14 mm thick. Two series of specimens were prepared for punching tests (series A and B). The specimens of series A were left for 4 da to allow for spring back then shaved into 12-mm-diameter circular dowels using a lathe. The specimens in series B were shaved into 12-mm-diameter round dowels right after completion of the hot-press process. Parent specimens of spruce 75 × 75 mm^2 were then prepared with 12-mm-diameter center holes longitudinal to the grain. Water was injected into the hole before the dowels were inserted.

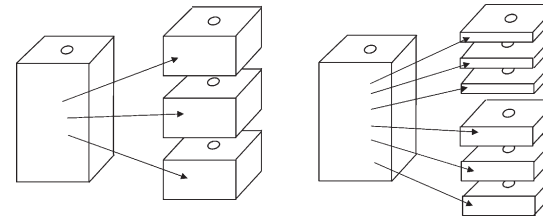

Figure 6. Punching shear specimen slicing preparation for 10-, 20-, and 30-mm-thick specimens.

This resulted in two different levels of swelling of hot-pressed dowels.

The completed samples were then sliced into punching shear specimens (Fig 6). Thicknesses tested included 10, 20, 30, 50, 80, 100, and 150 mm. A total of five tests were conducted for each thickness group, which makes up 70 specimens for punching tests. The specimens were left 4 da before testing to allow the dowels to dry.

The punching shear tests were conducted using a customized rig and a 100-kN test machine at a rate of 0.5 mm/min. Tests were conducted up to the point at which the dowel was completely punched out or up to a 10-mm slip displacement. The overall test set-up is illustrated in Fig 7.

Time-Dependent Shear Tests

To investigate the relationship between shear strength and time, a series of punching shear tests were carried out on Type B specimens 2, 48, 168, 720, and 2160 h after the specimens were prepared. Specimens were 10 mm thick, and five specimens were tested for each time span. This series of specimens were tested with the same conditions as punching shear tests.

Beam Tests

A hot-pressed dowel was used to connect two pieces of timber with dimensions of 75 × 150 × 600 mm^3 to build a 1.2-m-long beam. A total of 24 specimens were fabricated for bending tests. Grade C16 European whitewood (*Picea abies*) was used as the parent beam material. Embedment length was kept constant at 100 mm each end (200 mm total dowel length). The average

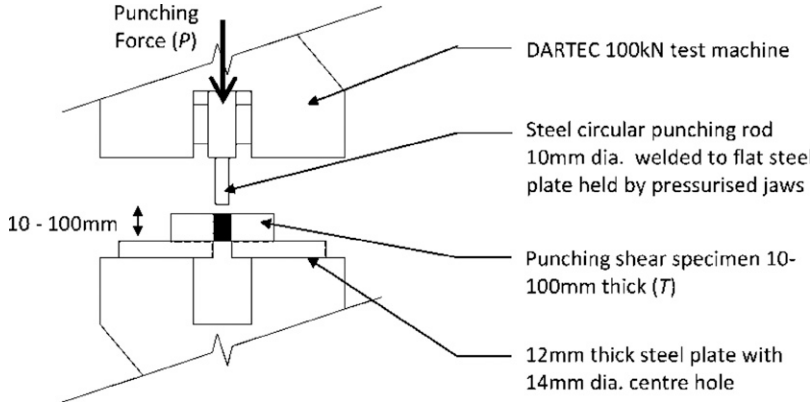

Figure 7. Punching shear test set-up.

moisture content of the beam specimens was 12%, measured by moisture meter before the tests.

Factors investigated in this study include edge distance and types of dowels. The edge distance is defined as the distance from the beam soffit to the placement of the dowel center within the section. The edge distances tested included 2*d* (24 mm), 3*d* (36 mm), 4*d* (48 mm), and 5*d* (60 mm), in which *d* is the dowel diameter. Two types of dowels, as explained in the punching shear tests section, were used to connect beam specimens. Three repetitions were tested with each factor combination. Table 1 gives the name and details of each specimen. The specimens and the test set-up are shown in Fig 8.

Table 1. Parameters for beam bending tests.

Specimens	Type of dowel[a]	Edge distance	No. of specimens
A-2d	A	2*d*	3
A-3d	A	3*d*	3
A-4d	A	4*d*	3
A-5d	A	5*d*	3
B-2d	B	2*d*	3
B-3d	B	3*d*	3
B-4d	B	4*d*	3
B-5d	B	5*d*	3

[a] A indicates the same process of dowels in group A in punching shear tests, whereas B indicates the B group.

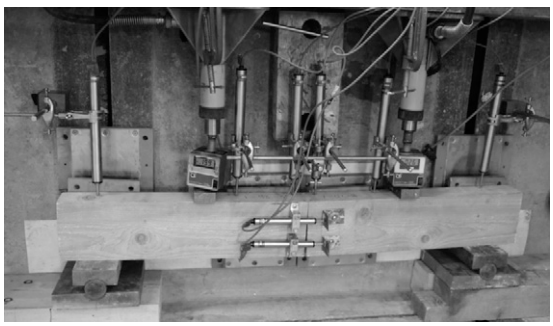

Figure 8. Beam bending test set-up.

RESULTS AND DISCUSSION

Bending Tests

The results of bending tests have shown an average modulus of elasticity (MOE) of 13.86 kN/mm^2 with a standard deviation of 0.41 kN/mm^2, which is comparable with timber of strength class C35 ($E_{0,\text{mean}} = 13$ kN/mm^2). Based on BSI (2007), the 5% MOE ($E_{0.05}$) is 12.81 kN/mm, which is comparable with timber of strength class C50 (11 kN/mm^2). This shows that MOE has increased by two times compared with strength class C16 after the hot-pressed process and also demonstrates that the hot-press process can be a useful method to enhance the mechanical properties of low-grade timber.

The results also showed that the hot-press process significantly increased bending strength of low-grade timber. The characteristic bending strength of the hot-pressed timber was 66.5 kN/mm^2, which is greater than the characteristic bending strength of C50 timber and comparable with D60 hardwood.

Punching Shear Tests

The results of punching shear tests are summarized in Table 2, and Fig 9 plots the maximum shear stress against specimen thickness. Maximum average shear stress was calculated by

$$\tau_{av,peak} = \frac{P_{max}}{\pi \cdot d \cdot l} \quad (17)$$

where P_{max}, d, and l are peak force when dowels are mobilized, the diameter of dowel, and the length of dowel, respectively. Specimens in series B showed much higher peak values, which consequently led to greater average maximum shear stresses. This was because the series B hot-pressed dowels did not spring back before they were inserted into the holes in beam members. The swelling started because of water in the holes after dowels were inserted into and confined by the holes. In comparison, the dowels in series A sprang back before they were shaved into dowels; therefore, exhibiting limited swelling even with being soaked in water in the holes of beam members.

Initially, maximum average shear stress was found to decrease rapidly as specimen thickness increased, but this relationship started leveling off near 100 mm for series A dowels and 50 mm for series B dowels. After these thickness levels, there were no significant decreases in maximum average shear stress. This is compliant with existing bonded-in rod theory (Volkersen 1953).

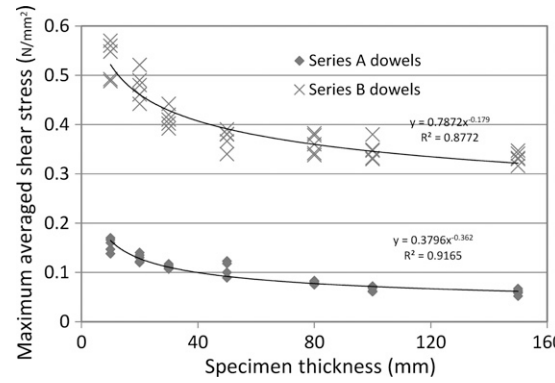

Figure 9. Average shear stress at peak load vs specimen thickness.

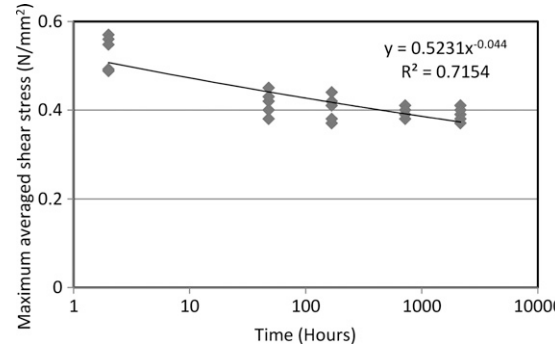

Figure 10. Average shear stress at peak load of 10-mm-thick specimens vs time after fabrication.

Time-Dependent Shear Strength

The friction between dowels and parent timbers relies on swelling of compressed wood. Therefore, drying of dowels and parent timbers influences the punching shear with time. Figure 10 depicts the relationship between shear strength and time after the specimens were fabricated. It shows that average punching shear strength of the specimens decreased with time. However, 2 da after the specimens were prepared, shear

Table 2. Results for punching shear tests.

Specimen series	Average P_{max} (N)[a]	Maximum average shear stress, $\tau_{av,peak}$ (N/mm^2)[a]	Specimen series	Average P_{max} (N)[a]	Average maximum shear stress, $\tau_{av,\ peak}$ (N/mm^2)[a]
A-10	58.89 (5.05)	0.156 (0.013)	B-10	200.41 (14.62)	0.532 (0.039)
A-20	97.57 (6.39)	0.129 (0.008)	B-20	361.01 (22.55)	0.479 (0.030)
A-30	125.99 (4.70)	0.111 (0.004)	B-30	467.32 (21.61)	0.413 (0.019)
A-50	199.81 (26.56)	0.106 (0.014)	B-50	700.07 (36.83)	0.371 (0.020)
A-80	237.05 (10.14)	0.079 (0.003)	B-80	1085.73 (60.62)	0.360 (0.020)
A-100	251.08 (18.39)	0.067 (0.005)	B-100	1310.42 (75.52)	0.348 (0.020)
A-150	339.29 (31.74)	0.060 (0.006)	B-150	1884.20 (66.84)	0.333 (0.012)

[a] Standard deviation is shown in parentheses.

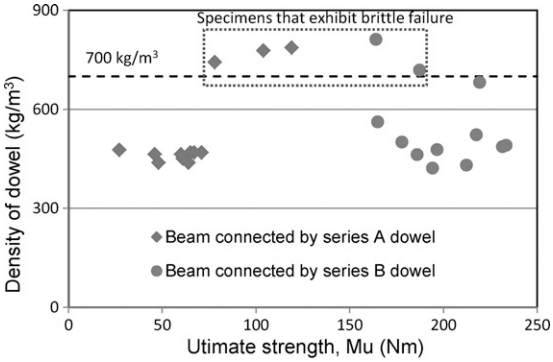

Figure 11. Density of hot-pressed dowel vs ultimate bending capacity of beam.

strength did not show any significant changes. Shear strength of the specimens was 0.42 and 0.39 N/mm^2 for 2 da and 90 da after fabrication, respectively. These represent 22% and 27% reductions when compared with 2-h observations after the specimens were made.

Beam Bending Tests

Two different failure modes occurred in the beam tests, brittleness and ductile failures. Observations from experimental results showed that 9 out of 12 beam specimens connected with series A dowels and 10 out of 12 specimens connected with series B dowels exhibited ductile failure. This implies that beams connected with hot-pressed dowels normally fail in ductile mode, which is usually preferred for a structural application to avoid catastrophic collapse of structures.

Specimens that failed in a ductile manner appeared to partially snap forming an intact hinge at peak moment. Postpeak, the connection showed about half the moment capacity when the dowel appeared to provide purely frictional resistance by sliding out of the clearance holes. The ductility appeared to be provided by this frictional resistance, a large portion of which was caused by swelling of the dowel. This was particularly obvious when the beam specimens were connected by series B dowels. This also indicates that more swelling provided greater postpeak residual strength.

Brittle specimens typically had higher moment capacities than that of a ductile counterpart. In this case, the dowel did not form a hinge and suddenly snapped at the maximum moment capacity, showing no postpeak ductility.

Dowel density was measured before the tests, and it was found that the denser dowels were responsible for the brittle specimen failures. This means that using denser dowels will lead to more brittle failures because of the inability to form early hinges and access the residual frictional resistance. All dowels were taken from the same piece of timber. Therefore, these differences in density may have been caused by the presence of juvenile wood along the timber length. Figure 11 plots the ultimate strength of beams connected by the two series of dowels against the density of the dowels. Those specimens connected by dowels with density greater than 700 kg/m^3 exhibited failure in the brittle manner. For structural applications, lower density dowels (less than 700 kg/m^3) will help to ensure a ductile failure. A quality control procedure will also be required to monitor dowel

Table 3. Results for beam tests.[a]

Specimens	Ultimate strength M_{ult} (Nm)	Initial rotational stiffness k_i (kNm/rad)	Rotation at peak moment θ_{peak} (rads)	Rotation at failure $\theta_{failure}$ (rads)
A-2d	84.67 (29.94)	2.76 (3.08)	0.14 (0.07)	0.27 (0.05)
A-3d	58.00 (8.89)	2.78 (1.46)	0.11 (0.04)	0.34 (0.04)
A-4d	72.33 (29.37)	1.01 (0.34)	0.16 (0.12)	0.34 (0.04)
A-5d	55.00 (25.87)	0.75 (0.33)	0.25 (0.13)	0.37 (0.02)
B-2d	227.48 (8.68)	6.32 (1.03)	0.18 (0.06)	0.33 (0.04)
B-3d	206.26 (16.85)	5.87 (1.52)	0.16 (0.02)	0.36 (0.01)
B-4d	192.27 (5.57)	3.63 (0.73)	0.20 (0.08)	0.29 (0.06)
B-5d	168.88 (7.73)	2.88 (0.47)	0.14 (0.04)	0.26 (0.03)

[a] Standard deviation is shown in parentheses.

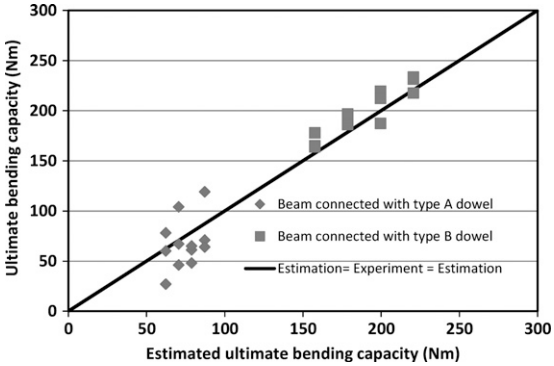

Figure 12. Comparison of results from estimation and experiments.

density before and after hot pressing, which can fluctuate substantially (Kitamori et al 2010).

Table 3 summarizes the beam test results, which shows maximum moment capacity, initial rotational stiffness, rotation at peak, and rotation at failure. The results show that the smaller the edge distances, the greater ultimate strength the beam had. The beams connected by series B dowels had significantly greater ultimate strength compared with those connected by series A dowels. This also reflects the fact that the punching shear strengths of series B dowels were greater than those of series A dowels. These two phenomena will be subsequently explained in the analytical model.

Comparison with Analytical Model

The analytical model was developed earlier in this study using the energy method. The moment capacity of beams can be calculated with Eq 15. Comparisons between estimated strength and those obtained from experiments are given in Fig 12. Satisfactory agreement was found between analytical and experimental results. Beams connected with type A dowels had more errors than those with type B dowels.

CONCLUSIONS

The proposed connection system was used in a beam splice connection. Bending tests were carried out to assess its performance in a practical application. Modest moment capacities in the region of 0.055-0.085 and 0.16-0.24 kNm occurred for specimens with type A and type B dowels, respectively. All specimens showed very high rotations at failure at about 0.30-0.35 radians (17-20°), which is favorable for structural applications to provide early precollapse warning.

REFERENCES

Ansell M, Smedley D (2007) Briefing: Bonded-in technology for structural timber. Proc ICE-Construction Materials 160(3):95-98.

Anshari B, Guan Z, Kitamori A, Jung K, Hassel I, Komatsu K (2011) Mechanical and moisture-dependent swelling properties of compressed Japanese cedar. Construct Build Mater 25(4):1718-1725.

Anshari B, Guan Z, Kitamori A, Jung K, Komatsu K (2012) Structural behaviour of glued laminated timber beams pre-stressed by compressed wood. Construct Build Mater 29:24-32.

Bainbridge R, Mettem C (1999) Bonded-in rods for timber structures: A versatile method for achieving structural connections. Struct Eng 77(15):24-27.

Blass H, Laskewitz B (1999) Effect of spacing and edge distance on the axial strength of glued-in rods. CIB-W18 Meeting 32 Graz, Austria, Universität Karlsruhe.

BSI (2007) BS EN 14358:2006 Timber structures: Calculation of characteristic 5-percentile values and acceptance criteria for a sample. British Standards Institute, London.

BSI (2011) BS EN 408: 2010 Timber structures: Structural timber and glued laminated timber—determination of some physical and mechanical properties. British Standards Institute, London.

Fang C-H, Mariotti N, Cloutier A, Koubaa A, Blanchet P (2012) Densification of wood veneers by compression combined with heat and steam. European Journal of Wood and Wood Products 70(1-3):155-163.

Feligioni L, Lavisci P, Duchanois G, De Ciechi M, Spinelli P (2003) Influence of glue rheology and joint thickness on the strength of bonded-in rods. Holz Roh Werkst 61(4):281-287.

Gustafsson P, Serrano E, Aicher S, Johansson C (2001) A strength design equation for glued-in rods. In Proc International RILEM Symposium on Joints in Timber Structures, RILEM (International Union of Laboratories and Experts in Construction Materials, Systems and Structures), Stuttgart, Germany.

Harvey K, Ansell MP (2003) Improved timber connections using bonded-in GFRP rods, PhD Thesis, University of Bath, UK.

Jensen J, Koizumi A, Sasaki T, Tamura Y, Iijima Y (2001) Axially loaded glued-in hardwood dowels. Wood Sci Technol 35(1-2):73-83.

Jung K, Murakami S, Kitamori A, Chang W-S, Komatsu K (2010) Improvement of glued-in-rod joint system

using compressed wooden dowel. Holzforschung 64(6): 799-804.

Kitamori A, Jung K, Mori T, Komatsu K (2010) Mechanical properties of compressed wood in accordance with the compression ratio. Mokuzai Gakkaishi 56(2):67-78 [in Japanese].

Rautkari L, Properzi M, Pichelin F, Hughes M (2010) Properties and set-recovery of surface densified Norway spruce and European beech. Wood Sci Technol 44(4): 679-691.

Steiger R, Gehri E, Widmann R (2007) Pull-out strength of axially loaded steel rods bonded in glulam parallel to the grain. Mater Struct 40(1):69-78.

Volkersen O (1953) Die Schubkraftverteilung in Leim-, Niet- und Bolzenverbindungen. Energie Technik 5(68):103.

Welzbacher C, Wehsener J, Rapp A, Haller P (2008) Thermo-mechanical densification combined with thermal modification of Norway spruce (*Picea abies* Karst) in industrial scale—Dimensional stability and durability aspects. Holz Roh Werkst 66(1):39-49.

Yeboah D, Gilbert S, Gilfillan R (2009) The behaviour of moment-resisting timber joints using bonded steel rods. In Proc 11th International Conference on Non-conventional Materials and Technologies (NOCMAT), Bath, UK.